Pulsed-Potential Electrochemical Reduction of Nitrate to Ammonia.

Sarah Mokhatrish, Naveen Halappa, Yun Hau Ng

Department of Chemical Engineering, Physical Science and Engineering (PSE) Division

King Abdullah University of Science and Technology (KAUST)

Abstract

Nitrate contamination of ground and industrial waters is a growing environmental concern, and its electrochemical reduction offers a route to close the nitrogen cycle while producing ammonia (NH_3) under ambient conditions, avoiding the energy- and carbon-intensive Haber–Bosch process. In this project, cuprous oxide (Cu_2O) nanoparticles were synthesized by a wet-chemical L-ascorbic acid reduction route and processed through washing, vacuum drying, calcination, ink formulation, and spray coating onto carbon paper to fabricate working electrodes for the electrocatalytic nitrate reduction reaction (NO_3RR). Both the as-prepared (uncalcined) and calcined catalysts were evaluated in an alkaline flow-cell configuration (1.0 M KOH with 0.1 M KNO_3). Linear sweep voltammetry showed a marked increase in cathodic current in the presence of nitrate for both catalyst forms relative to their respective KOH-only blanks, with the uncalcined electrode exhibiting substantially higher overall current density. Scanning electron microscopy confirmed that the nanoparticulate morphology was retained after calcination, X-ray diffraction matched the cubic Cu_2O (cuprite) reference pattern (JCPDS 00-005-0667), and energy-dispersive X-ray spectroscopy of the calcined catalyst gave a composition of 87.8% Cu and 12.2% O, consistent with stoichiometric Cu_2O. Ammonia formation, quantified by the indophenol blue UV–Vis method and independently confirmed by ^1H NMR (three characteristic NH_4^+ peaks at δ 7.06, 7.00, and 6.95 ppm), was observed across the applied potential window of −1.3 to −1.9 V vs. Ag/AgCl for both catalysts, with Faradaic efficiency values reaching 80.12% (calcined) and 78.78% (uncalcined), each peaking at −1.6 V. In addition to constant-potential electrolysis, a pulsed electrolysis protocol (alternating between −1.3 to −1.7 V for 4 s and 0.4 V for 1 s vs. Ag/AgCl) was also explored as a complementary operating strategy. These results support Cu_2O — in both its calcined and uncalcined forms — as a promising, low-cost catalyst platform for coupling ammonia electrosynthesis with nitrate remediation.

Date: August 2026

Institution: King Abdullah University of Science and Technology (KAUST)

Host Program: KAUST Academy Cooperative Training — Physical Science and Engineering (PSE) Division

1. Introduction

Ammonia (NH_3) is a foundational chemical feedstock, underpinning the production of fertilizers, synthetic fibers, and a wide range of industrial and pharmaceutical products. It is also increasingly considered a carbon-free hydrogen carrier owing to its high energy density and ease of storage relative to molecular hydrogen. Industrially, ammonia is produced almost exclusively via the Haber–Bosch process, which operates at high temperature and pressure using hydrogen typically derived from methane reforming, resulting in substantial energy consumption and carbon dioxide emissions.

At the same time, decades of intensive nitrogen fertilizer use and industrial discharge have led to a significant accumulation of nitrate (NO_3^-) and nitrite (NO_2^-) in groundwater and wastewater streams. These nitrogen oxyanions pose recognized risks to aquatic ecosystems and human health. The electrochemical reduction of nitrate to ammonia (NO_3RR) has therefore emerged as an attractive dual-purpose strategy: it enables decentralized, renewable-energy-powered ammonia synthesis while simultaneously remediating nitrate-contaminated water.

Copper-based materials are among the most promising electrocatalysts for NO_3RR because of their low cost, relatively high selectivity toward ammonia, and moderate overpotential requirements. Among these, cuprous oxide (Cu_2O) has attracted particular interest as a precatalyst: under cathodic bias, Cu_2O undergoes progressive electrochemical reduction toward metallic copper, and the evolving Cu(I)/Cu(0) speciation has been directly correlated with the catalytic selectivity toward nitrite versus ammonia in the literature. This project builds on that understanding by synthesizing Cu_2O nanoparticles in-house, fabricating flow-cell electrodes from both the as-prepared and calcined catalyst, and comparing their performance toward electrocatalytic nitrate reduction to ammonia.

2. Literature Background

Recent mechanistic studies on Cu_2O-based nanocatalysts have shown that the chemical state of copper dynamically evolves under applied cathodic potential, and that this evolution governs product selectivity. Using combined quasi in situ X-ray photoelectron spectroscopy and operando X-ray absorption spectroscopy, Bai et al. demonstrated that Cu(I) species predominate during the initial two-electron reduction of nitrate to nitrite at low overpotentials, whereas metallic Cu(0) becomes the dominant surface species at more cathodic potentials, correlating strongly with high Faradaic efficiency toward ammonia [1]. Their electrokinetic analysis further indicated that the rate-determining step of NO_3RR at low overpotential is a proton-coupled electron transfer involving adsorbed nitrate, and that hydroxylamine (NH_2OH) is a key intermediate on the pathway to ammonia [1].

Beyond pure Cu_2O, doping and compositing strategies have also been explored to enhance NO_3RR performance. For example, Dai et al. reported that incorporating copper into a CeO_2 lattice via electrodeposition increased the oxygen vacancy concentration of the oxide, providing additional active sites and enhancing internal charge transfer; the resulting Cu–CeO_2 solid solution achieved a substantially higher ammonia yield and Faradaic efficiency than bare CeO_2 [2]. Together, these studies motivate the use of Cu_2O nanostructures as a well-defined, low-cost model catalyst system for probing structure–activity relationships in electrocatalytic nitrate reduction, which is the approach adopted in the present project — extended here to a direct comparison of the as-prepared (uncalcined) and calcined forms of the catalyst.

3. Project Objectives

- Synthesize Cu_2O nanoparticles via a wet-chemical L-ascorbic acid reduction route and process them (washing, vacuum drying, calcination) into catalysts suitable for electrode fabrication.
- Fabricate spray-coated Cu_2O electrodes on carbon paper, using both the as-prepared and calcined catalyst, and assemble them into a flow-cell electrochemical system for nitrate reduction testing.
- Characterize the structural, morphological, and compositional properties of the as-prepared and calcined catalyst using SEM, EDX, and XRD.
- Evaluate and compare the electrocatalytic activity of the uncalcined and calcined Cu_2O electrodes toward nitrate reduction using linear sweep voltammetry, and toward ammonia formation using chronoamperometric electrolysis.
- Quantify the ammonia reaction product via UV–Vis spectrophotometry (indophenol blue method) and determine the Faradaic efficiency and concentration of ammonia as a function of applied potential for both catalyst forms.
- Independently confirm the identity of the ammonia/ammonium product by ^1H NMR spectroscopy.

4. Experimental Methodology

The experimental workflow followed a nine-step sequence, illustrated schematically in Figure 1: catalyst synthesis, washing and centrifugation, vacuum drying, calcination, catalyst ink preparation, electrode spray coating, electrochemical cell assembly, electrochemical measurement, and final product quantification by UV–Vis spectroscopy.

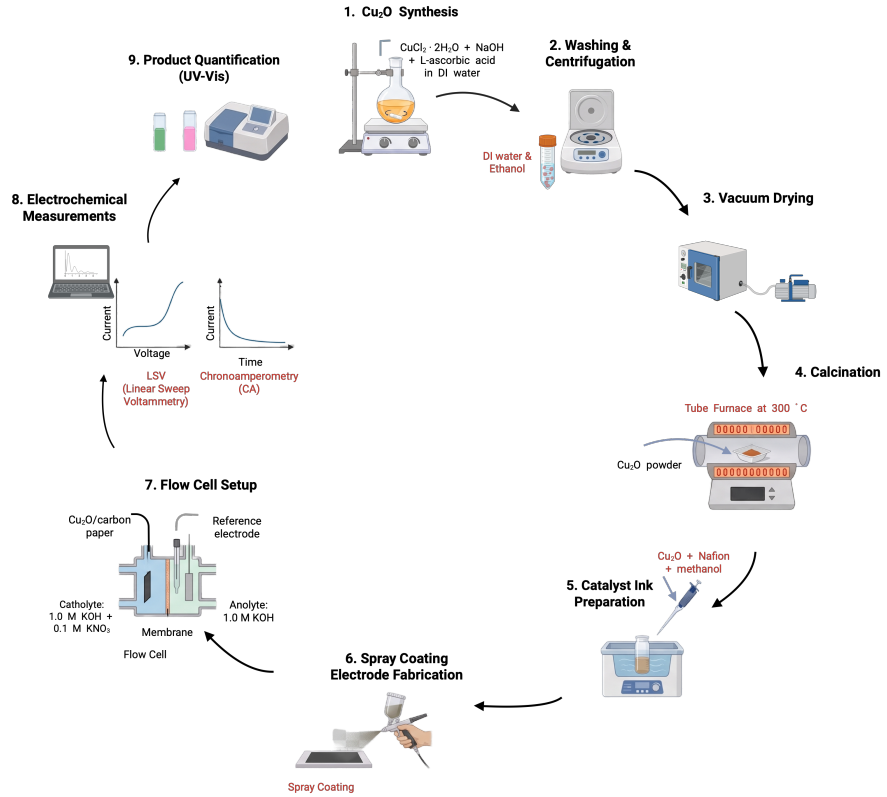


Figure 1. Overview of the nine-step experimental workflow, from Cu_2O synthesis to electrochemical product quantification.

4.1 Materials

Copper(II) chloride dihydrate ($CuCl_2 \cdot 2H_2O$), sodium hydroxide (NaOH), and L-ascorbic acid were used as received for catalyst synthesis in deionized (DI) water. Nafion solution and methanol were used for catalyst ink preparation, with carbon paper as the electrode support. For electrochemical testing, potassium hydroxide (KOH) and potassium nitrate (KNO_3) were used to prepare the catholyte (1.0 M KOH + 0.1 M KNO_3) and anolyte (1.0 M KOH).

4.2 Catalyst Synthesis

Cu_2O nanoparticles were synthesized by a surfactant-free wet-chemical reduction method. $CuCl_2 \cdot 2H_2O$ and NaOH were dissolved in DI water under stirring, and a freshly prepared L-ascorbic acid solution was subsequently added as the reducing agent. The mixture was stirred for 1 h at room temperature, during which the solution progressively developed a precipitate characteristic of Cu_2O formation. The as-formed precipitate was recovered by centrifugation and washed repeatedly with DI water and ethanol to remove unreacted precursors and reaction by-products. The washed solid was then dried under vacuum to remove residual solvent.

4.3 Calcination

A portion of the dried Cu_2O powder was calcined under a flowing nitrogen atmosphere at 300 °C for 300 min (5 h), using a ramp rate of 3 °C min^{-1}. This thermal treatment step was applied to assess its effect on catalyst crystallinity, morphology, and electrocatalytic performance relative to the as-prepared (uncalcined) catalyst, as evaluated by SEM, XRD, and electrochemical testing (Section 6).

4.4 Catalyst Ink Preparation and Spray Coating

The Cu_2O catalyst — both the as-prepared and calcined forms — was dispersed in methanol together with Nafion solution as a polymeric binder. Each suspension was ultrasonicated for 1 h to yield a uniform, well-dispersed catalyst ink. The ink was then deposited onto carbon paper using a spray-coating technique to form the catalyst layer of the working electrode. The coated electrodes were dried at room temperature prior to assembly into the electrochemical cell.

4.5 Electrochemical Cell Setup

The primary electrocatalytic testing reported in this work used a flow-cell configuration, in which the electrolyte (1.0 M KOH + 0.1 M KNO_3 catholyte; 1.0 M KOH anolyte, controlled flow) was continuously supplied to the Cu_2O-on-carbon-paper electrode, improving mass transport of nitrate to the catalyst surface relative to a static cell.

4.6 Electrochemical Measurements

Electrochemical characterization included linear sweep voltammetry (LSV) and chronoamperometry (CA). LSV was used to compare the cathodic polarization behavior of the uncalcined and calcined Cu_2O electrodes in 1.0 M KOH alone and in 1.0 M KOH with 0.1 M KNO_3, in order to identify the potential window over which nitrate reduction becomes active relative to the competing hydrogen evolution reaction (HER). Chronoamperometric electrolysis was subsequently performed at a series of fixed potentials (−1.3 to −1.9 V vs. Ag/AgCl) to generate reaction products for quantification.

In addition to constant-potential electrolysis, a pulsed electrolysis protocol was also employed as a complementary operating strategy (Figure 2). In this protocol, the applied potential was cycled repeatedly between a cathodic pulse in the range −1.3 to −1.7 V (vs. Ag/AgCl), matching the potentials investigated under

constant-potential operation, held for 4 s, and a relaxation potential of 0.4 V held for 1 s, with the cycle repeated continuously for a total electrolysis time of 900 s. This pulsed approach was explored to assess whether periodically interrupting the cathodic bias could help maintain nitrate mass transport to the electrode surface and mitigate the build-up of reduction intermediates during extended electrolysis, relative to operation at a single constant potential.

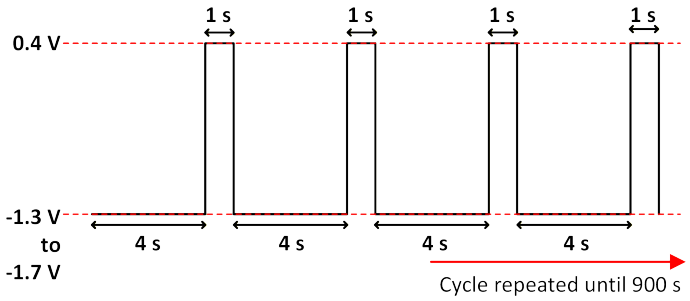


Figure 2. Pulsed electrolysis waveform, alternating between a cathodic pulse (−1.3 to −1.7 V vs. Ag/AgCl) for 4 s and a relaxation potential of 0.4 V for 1 s, repeated cyclically for a total of 900 s.

5. Characterization Techniques

A combination of structural, morphological, and spectroscopic techniques was used to characterize the Cu_2O catalyst before and after calcination, and to quantify and confirm the products of the electrocatalytic nitrate reduction reaction.

5.1 Scanning Electron Microscopy (SEM)

Field-emission scanning electron microscopy (FESEM) was used to examine the morphology and surface structure of the Cu_2O nanoparticles, both as-prepared and after calcination (Section 6.1, Figure 3).

5.2 Energy-Dispersive X-ray Spectroscopy (EDX)

EDX analysis was performed on the calcined Cu_2O nanoparticles to assess elemental composition. The measured composition was 87.8 wt% Cu and 12.2 wt% O, in close agreement with the theoretical mass fraction of stoichiometric Cu_2O (88.8% Cu, 11.2% O), supporting the phase purity indicated independently by XRD.

5.3 X-ray Diffraction (XRD)

Powder X-ray diffraction was performed on the as-prepared (uncalcined) Cu_2O nanoparticles to identify the crystalline phase(s) present. The diffractogram (Section 6.2, Figure 4) was indexed against the reference pattern for cubic Cu_2O (cuprite, JCPDS 00-005-0667).

5.4 Nuclear Magnetic Resonance (NMR)

^1H NMR spectroscopy was used to independently confirm the chemical identity of the nitrogen-containing electrolysis product, complementing the UV–Vis colorimetric assay (Section 6.5, Figure 8).

5.5 UV–Vis Spectrophotometry

UV–Vis spectrophotometry was used to quantify ammonia, the principal reaction product of NO_3RR reported in this work, using the indophenol blue method with absorbance measured at 655 nm (the Griess method for nitrite, with absorbance measured at 540 nm, was also available as part of the analytical workflow but was not used for

the quantitative results presented here). A calibration curve was constructed from standard solutions of known NH_3 concentration, and the resulting linear fit ($y = 0.3791x + 0.009$, $R^2 = 0.9999$) was used to convert measured sample absorbance into product concentration and Faradaic efficiency. The corresponding standard spectra and calibration curve are presented in Sections 6.6 and 6.7.

6. Results

6.1 Morphology (SEM)

Figure 3 shows FESEM images of the Cu_2O nanoparticles (a) as-prepared (uncalcined) and (b) after calcination at 300 °C. In both cases, the catalyst consists of densely packed, well-defined nanoparticulate/nanocube features with no evidence of gross sintering or loss of the nanostructured morphology after the thermal treatment. The calcined sample (imaged at higher magnification, 100,000×) shows individual cubic and sub-cubic particle facets more clearly, while retaining the same general particle packing observed for the uncalcined sample. This is consistent with the calcination step primarily affecting crystallinity and phase character rather than causing significant morphological coarsening.

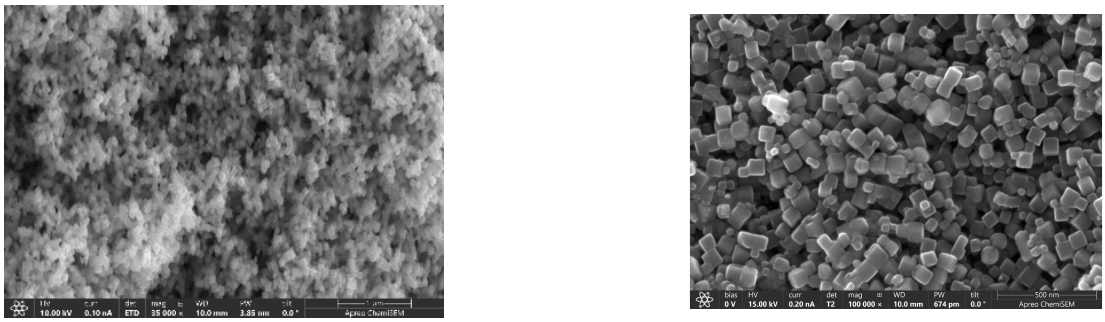


Figure 3. FESEM images of (a) as-prepared (uncalcined) Cu_2O nanoparticles (35,000×, 10.00 kV) and (b) Cu_2O nanoparticles after calcination at 300 °C for 5 h under N_2 (100,000×, 15.00 kV).

6.2 Crystal Structure (XRD)

The XRD pattern of the as-prepared Cu_2O catalyst (Figure 4) exhibits sharp diffraction peaks at approximately 29.6°, 36.4°, 42.3°, 52.5°, 61.4°, 69.6°, and 73.5° 2θ, which index respectively to the (110), (111), (200), (211), (220), (311), and (222) reflections of cubic Cu_2O (cuprite phase, JCPDS 00-005-0667). The (111) reflection at 36.4° is the most intense peak, consistent with the expected relative intensities for the cuprite structure. No diffraction peaks attributable to metallic Cu(0) or CuO were observed, indicating that the as-prepared catalyst is phase-pure Cu_2O within the detection limit of the measurement.

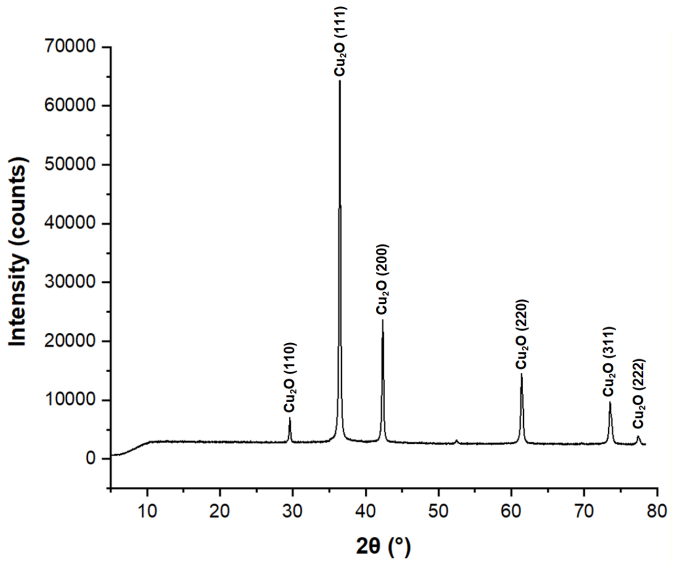


Figure 4. XRD pattern of the as-prepared (uncalcined) Cu_2O nanoparticles, with reflections indexed to cubic Cu_2O (cuprite, JCPDS 00-005-0667).

6.3 Electrochemical Activation of Nitrate (LSV)

Figure 5 compares linear sweep voltammograms of the calcined and uncalcined Cu_2O electrodes in 1.0 M KOH alone (blank) and in 1.0 M KOH with 0.1 M KNO_3. For both catalyst forms, the cathodic current is clearly enhanced in the nitrate-containing electrolyte relative to the corresponding KOH-only blank, confirming that nitrate activation occurs on both the uncalcined and calcined catalyst. The uncalcined electrode reaches substantially higher current densities than the calcined electrode under both blank and nitrate-containing conditions — for example, approaching −250 mA cm^{-2} near −2.0 V in 1.0 M KOH, compared with approximately −65 mA cm^{-2} for the calcined electrode at the same potential — consistent with a higher electrochemically active surface area and/or a more readily reducible oxide phase prior to thermal treatment. The uncalcined electrode in nitrate-containing electrolyte also displays a distinct current peak near −1.9 V before the current partially recedes at more negative potentials, a feature not observed for the calcined sample; this may reflect a surface reduction/restructuring process, such as progressive Cu(I)-to-Cu(0) conversion, that proceeds differently on the less thermally treated catalyst.

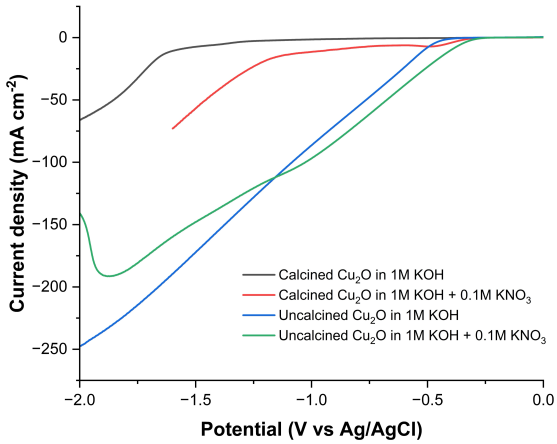


Figure 5. Linear sweep voltammograms of the calcined and uncalcined Cu_2O electrodes in 1.0 M KOH (with and without 0.1 M KNO_3).

6.4 Ammonia Faradaic Efficiency and Concentration

Chronoamperometric electrolysis was carried out at fixed potentials between −1.3 and −1.7 V vs. Ag/AgCl for both the calcined and uncalcined Cu_2O electrodes, and the resulting electrolyte was analyzed by UV–Vis spectrophotometry to determine the NH_3 Faradaic efficiency and concentration (Figures 6 and 7). For the calcined catalyst (Figure 6), the Faradaic efficiency increased from approximately 58% at −1.3 V to a maximum of 80.12% at −1.6 V, before decreasing at −1.7 V; the NH_3 concentration increased approximately monotonically, reaching a maximum of 3.32 mmol L^{-1} at −1.6 V. For the uncalcined catalyst (Figure 7), the trend was qualitatively similar: Faradaic efficiency rose from approximately 49% at −1.3 V to a maximum of 78.78% at −1.6 V, then decreased at −1.7 V, while the NH_3 concentration increased from ≈1.1 to a maximum of 3.606 mmol L^{-1} at −1.6 V.

Comparing the two catalyst forms, the calcined and uncalcined electrodes achieved a very similar peak Faradaic efficiency for ammonia (80.12% and 78.78%, respectively) at the same optimal potential of −1.6 V vs. Ag/AgCl. The uncalcined electrode, however, generated a somewhat higher peak NH_3 concentration (3.606 mmol L^{-1} versus 3.32 mmol L^{-1} for the calcined electrode), consistent with its higher overall current density observed in the LSV measurements (Section 6.3, Figure 5): more total charge is passed at a given potential, driving greater absolute product formation even though a comparable fraction of that charge is directed toward ammonia in both cases.

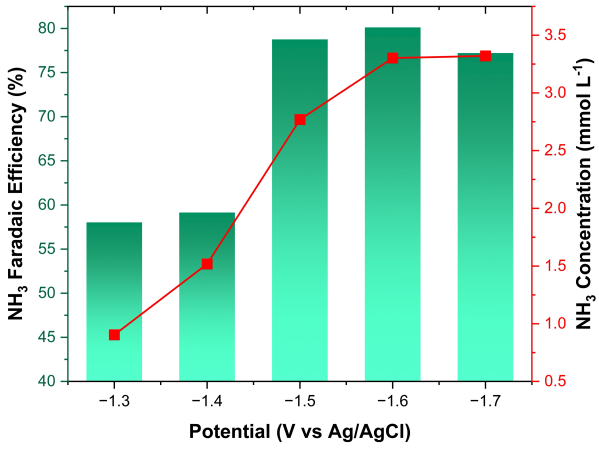


Figure 6. NH_3 Faradaic efficiency and concentration as a function of applied potential for the calcined Cu_2O electrode.

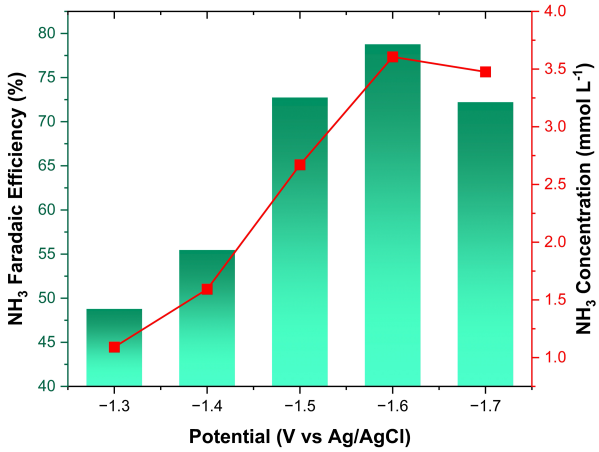


Figure 7. NH_3 Faradaic efficiency and concentration as a function of applied potential for the uncalcined Cu_2O electrode.

6.5 NMR Confirmation of Ammonium Formation

To independently confirm the chemical identity of the electrolysis product, ^1H NMR spectroscopy was performed on a representative post-electrolysis catholyte sample. The spectrum (Figure 8) shows a characteristic triplet centered at δ 7.06, 7.00, and 6.95 ppm, consistent with the ^1H–^{14}N spin-spin coupling pattern of the ammonium ion (NH_4^+). This result provides direct spectroscopic confirmation, independent of the UV–Vis colorimetric assay, that ammonium/ammonia is the nitrogen-containing product generated during nitrate reduction on the Cu_2O electrode.

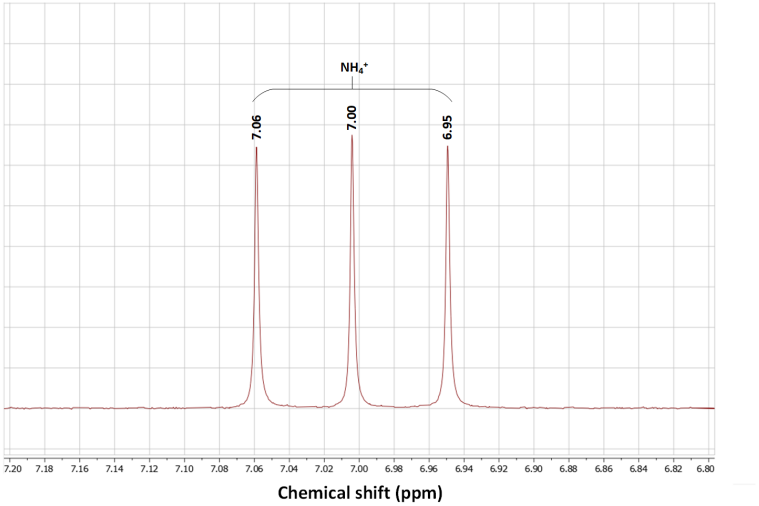


Figure 8. ^1H NMR spectrum of a post-electrolysis catholyte sample, showing the characteristic three-peak pattern of NH_4^+ at δ 7.06, 7.00, and 6.95 ppm.

6.6 Standard Calibration Spectra

Figure 9 shows the UV–Vis absorbance spectra of the standard solutions used to construct the NH_3 calibration curve. For NH_3 (indophenol blue method), standards ranging from 0.00 to 10.00 ppm were measured, showing a clear, concentration-dependent absorbance band centered at 655 nm. This standard spectral series forms the basis of the linear calibration fit presented in Section 6.7.

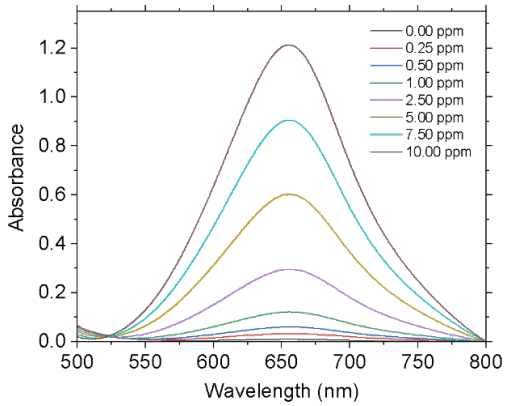


Figure 9. UV–Vis absorbance spectra of NH_3 standard solutions (0.00–10.00 ppm), indophenol blue method, λ_{max} = 655 nm.

6.7 Calibration Curve

Figure 10 shows the resulting linear calibration fit derived from the standard spectra in Figure 9, for NH_3 (indophenol blue method). The calibration exhibits excellent linearity (R^2 = 0.9999) over the tested concentration range, supporting its use for accurate ammonia quantification.

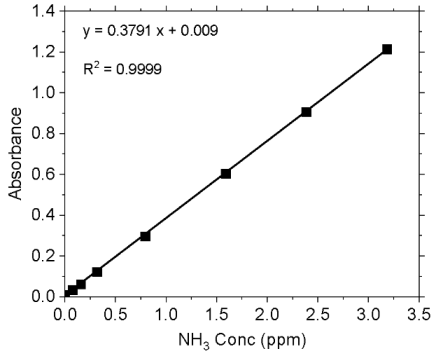


Figure 10. NH_3 calibration curve, indophenol blue method (λ = 655 nm), y = 0.3791x + 0.009, R^2 = 0.9999.

7. Discussion

The combination of SEM and XRD results indicates that Cu_2O nanoparticles with a well-defined nanocube morphology and a phase-pure cuprite structure were successfully synthesized, and that the nanoparticulate morphology is preserved after calcination at 300 °C. The EDX composition of the calcined catalyst (87.8% Cu, 12.2% O) is in close agreement with the stoichiometric value for Cu_2O, providing an independent compositional check that is consistent with the XRD phase assignment.

The LSV comparison (Figure 5) provides clear evidence that nitrate is activated on both the uncalcined and calcined Cu_2O electrode well ahead of the hydrogen evolution reaction, mirroring the behavior reported for Cu_2O nanocubes in alkaline nitrate-containing electrolyte, where the onset of the nitrate reduction wave occurs at considerably milder potentials than HER [1]. The markedly higher current density of the uncalcined electrode suggests that it presents a larger electrochemically active surface area, a more readily reducible surface, or both,

relative to the calcined catalyst — a reasonable outcome given that calcination is expected to increase crystallinity and could reduce surface defect density.

Despite this difference in overall current density, the calcined and uncalcined electrodes achieved a very similar peak Faradaic efficiency toward ammonia (80.12% and 78.78%, respectively), both maximized at −1.6 V vs. Ag/AgCl. This suggests that, once nitrate reduction is underway, the intrinsic selectivity of the Cu_2O-derived catalyst toward ammonia (as opposed to competing pathways such as HER or partial reduction to nitrite) is broadly similar for the two catalyst forms, even though the uncalcined electrode drives a larger absolute reaction rate (reflected in its higher NH_3 concentration at the optimal potential). The non-monotonic trend in Faradaic efficiency with applied potential — rising to a maximum near −1.6 V and then decreasing at −1.7 V for both catalysts — suggests that ammonia selectivity is governed by a balance of competing effects: at low overpotential, insufficient driving force may limit the multi-electron reduction steps required to convert nitrate/nitrite fully to ammonia, while at the most negative potentials tested, the competing hydrogen evolution reaction and/or mass-transport limitations of nitrate to the electrode surface may increasingly divert charge away from the ammonia-forming pathway. This interpretation is broadly consistent with mechanistic studies on Cu_2O nanocubes, which report that metallic Cu(0) — whose surface fraction increases with applied overpotential and electrolysis time — is the species primarily responsible for the multi-electron reduction of nitrate/nitrite to ammonia, while Cu(I) predominantly catalyzes the initial two-electron reduction of nitrate to nitrite [1].

The ^{1}H NMR spectrum (Figure 8) provides direct, independent confirmation of ammonium as the reaction product, corroborating the UV–Vis-based quantification and lending confidence to the Faradaic efficiency and concentration values reported in Section 6.4. Taken together, the structural, compositional, and electrochemical results indicate that both the calcined and uncalcined Cu_2O catalysts are active and reasonably selective toward electrocatalytic ammonia production from nitrate, with the choice between them representing a trade-off between raw current density/product concentration (favoring the uncalcined catalyst) and thermal/structural stabilization from calcination.

8. Challenges Encountered

- Achieving reproducible, uniform Cu_2O particle size and morphology across different synthesis batches required careful control of reagent addition order, stirring time, and precipitation conditions.
- Obtaining a uniform catalyst ink and a consistent, defect-free spray-coated catalyst layer on carbon paper was sensitive to ink dispersion quality and spray technique, and required repeated attempts to achieve reproducible electrode loading.
- Identifying calcination conditions that improved catalyst crystallinity without causing excessive particle agglomeration or morphological coarsening required care, given the limited number of calcination trials possible within the training period.
- Running and comparing electrochemical experiments and product analyses for two catalyst forms (calcined and uncalcined) across multiple applied potentials substantially increased the number of samples to prepare, test, and analyze within the available time.
- Ensuring reliable and reproducible NH_3 and NO_2^- quantification by UV–Vis required careful, consistent sample dilution and timing of the colorimetric reactions (indophenol blue and Griess methods) across many electrolysis samples.
- The limited duration of the training period and shared access to characterization instruments (SEM, XRD, EDX, NMR) constrained the number of repeat measurements and additional catalyst formulations that could be explored.

9. Future Work

- Further optimize Cu_2O synthesis conditions (reagent concentrations, addition rate, reaction temperature and time) to improve particle uniformity and batch-to-batch reproducibility.
- Systematically vary calcination temperature and duration to identify conditions that optimize the trade-off between crystallinity/stability and electrochemically active surface area.
- Improve catalyst loading control and spray-coating uniformity, for example through optimized ink rheology or automated coating equipment, to reduce electrode-to-electrode variability.
- Test additional flow-cell operating conditions, such as different KNO_3 concentrations, electrolyte pH, and flow rates, to further map the NO_3RR performance landscape.
- Perform additional characterization (e.g., XRD and SEM of the post-reaction electrodes, and X-ray photoelectron spectroscopy) to directly track structural and oxidation-state changes of the catalyst before and after electrolysis, complementing the ex situ characterization performed in this work.
- Conduct long-term stability and durability testing of both catalyst forms under continuous operation to assess practical viability.
- Pursue further optimization of the catalyst and operating conditions to maximize NH_3 selectivity while minimizing NO_2^- formation as a competing product.
- Study the relationship between Cu oxidation state, catalyst structure, and nitrate reduction performance in more detail, for example via operando spectroscopy, to build on the mechanistic framework established in the literature [1].

10. Conclusion

- Both uncalcined and calcined Cu_2O nanocubes showed effective nitrate-to-ammonia conversion.
- Although uncalcined Cu_2O exhibited a substantially higher cathodic current density in LSV, both catalysts achieved comparable NH_3 production (~3.3–3.6 mmol L^{-1}) and Faradaic efficiencies (~79–80%).
- Their optimum performance was observed at a negative potential of −1.6 V vs. Ag/AgCl.
- Calcination under N_2 preserved the Cu_2O nanocube morphology and cubic phase, indicating good structural stability during thermal treatment.
- A pulsed electrolysis protocol (alternating between −1.3 to −1.7 V for 4 s and 0.4 V for 1 s vs. Ag/AgCl) was also explored as a complementary approach to constant-potential electrolysis.
- Overall, these findings highlight Cu_2O nanocubes as a promising catalyst platform for electrochemical nitrate-to-ammonia conversion.

11. Acknowledgements

I would like to express my sincere gratitude to King Abdullah University of Science and Technology (KAUST) for providing the research facilities, resources, and training opportunity that made this project possible.

I am deeply grateful to my supervisor, Prof. Yun Hau Ng, for his guidance, insightful feedback, and continuous support throughout the course of this project.

I would also like to sincerely thank my mentor, Naveen Halappa, for his patient supervision, hands-on laboratory training, technical guidance, and constant encouragement throughout every stage of this work.

My thanks also extend to the members of the research group and laboratory for their assistance, helpful discussions, and collegial support during my time in the lab.

Finally, I gratefully acknowledge Imam Abdulrahman Bin Faisal University for supporting my participation in this cooperative training experience.

12. References

[1] Bai, L.; Franco, F.; Timoshenko, J.; Rettenmaier, C.; Scholten, F.; Jeon, H. S.; Yoon, A.; Rüscher, M.; Herzog, A.; Haase, F. T.; Kühl, S.; Chee, S. W.; Bergmann, A.; Cuenya, B. R. Electrocatalytic Nitrate and Nitrite Reduction toward Ammonia Using Cu_2O Nanocubes: Active Species and Reaction Mechanisms. J. Am. Chem. Soc. 2024, 146, 9665–9678.

[2] Dai, H.; Liu, L.; Zhao, H.; Zhou, P.; Ying, Y.; Yin, M.; Wang, X.; Fan, W.; Bai, H. Efficient Electrocatalytic Reduction of Nitrate to Ammonia Using Cu–CeO_2 Solid Solution. Int. J. Hydrogen Energy 2024, 73, 257–264.